# Methylene Substitution Reactions in a Quadrupole Ion Trap
## Selectivity of Ethylene, Ethylene Oxide, and Dimethyl Ether Reactive Ions

Tracy Donovan, Chien-Chung Liou, and Jennifer Brodbelt
Department of Chemistry and Biochemistry, University of Texas at Austin, Austin, Texas, USA

To elucidate the selectivity of methylene substitution reactions of monosubstituted and disubstituted oxyaromatic compounds in a low pressure quadrupole ion trap environment, the relative abundances of covalently bound and loosely bound adducts formed by ion/molecule reactions with ethylene (ET), ethylene oxide (ETOX), and dimethyl ether (DME) were compared. Adduct ions of all three reagent gases were formed in both a conventional ion source and a quadrupole ion trap and characterized by collisionally activated dissociation. For DME and ET, the covalently bound adducts formed at $(M + 45)^+$ and $(M + 41)^+$, respectively, are direct precursors to the methylene substitution product ions at $(M + 13)^+$. ETOX and ET do not demonstrate the same functional group selectivity for methylene substitution as previously observed for DME. This is attributed to differences in reaction exothermicities and competing reactions. *(J Am Soc Mass Spectrom 1992, 3, 39–46)*

Chemical ionization (CI) has gained widespread recognition as a selective and sensitive ionization technique [1–5]. The majority of studies utilizing CI have focused on reagents such as methane, isobutane, and ammonia that promote exothermic proton transfer reactions. However, newly explored reagents may also promote substitution, addition, and abstraction reactions, often with formation of structurally specific adducts. For example, several alternative reagents (methylamine [6], NO [7], and vinyl methyl ether [8]) have proven useful for locating the position of double bonds in olefins, whereas tetramethylsilane [9] has been used to probe the nature of aliphatic alcohols. Other CI reagents that have demonstrated analytical utility include ethylene oxide (ETOX) [10], acetone [11], various alkyl amines [12], dimethyl ether (DME) [13], and methylene chloride [14]. Recently it was shown that metal ions can be used as CI agents [15–18], and specifically to locate double bonds in olefins [17] and to distinguish isomers [18].

From a fundamental perspective, it is important to understand the mechanisms of CI and the details of the selectivity of ion/molecule reactions involved in adduct formation. Such an understanding can provide a basis for a rational approach to developing alternative CI agents. Although adduct formation with the alternative CI reagents mentioned above is commonly observed, the value of such species as diagnostic probes for substrate structure and mechanisms of ionization reactions has only recently begun to be addressed. For example, DME proved to have analytical value as a structurally specific CI reagent [19], but without an accompanying explanation for its selectivity. We present here an examination of other reactive gases that promote ion/molecule chemistry similar to that observed for DME but do not exhibit the desired selectivity. From a comparison of adduct formation and structural characterization by collisionally activated dissociation (CAD), a rationalization of the differences is obtained.

As just mentioned, we have evaluated DME as a selective CI reagent in both a conventional ion source and in a quadrupole ion trap, and it exhibited useful properties as an alternative ionization reagent for substituted aromatic compounds in the quadrupole ion trap [19]. The predominant reactive species from DME were $CH_3\overset{+}{O} = CH_2$ ($m/z$ 45) and $CH_3\overset{+}{O}HCH_3$ ($m/z$ 47). In a quadrupole ion trap mass spectrometer (ITMS), ion/molecule reactions of $CH_3\overset{+}{O} = CH_2$ with substituted aromatics resulted in formation of $(M + 13)^+$ or $(M + 15)^+$ adducts depending on the nature

Address reprint requests to Jennifer Brodbelt, Department of Chemistry and Biochemistry, University of Texas at Austin, Austin, TX 78712-1167.


1044-0305/92/$3.50

Received May 8, 1991
Revised June 26, 1991
Accepted June 26, 1991

of the substituent. It was determined that the $(M + 13)^+$ adduct resulted from $[M + (CH_3O = CH_2) - CH_3OH]^+$, whereas the $(M + 15)^+$ resulted from $[M + (CH_3O = CH_2) - CH_2O]^+$. Those aromatic compounds with an ether or alcohol function group, such as phenol or anisole, formed $(M + 13)^+$ ions, whereas those aromatic compounds with a carbonyl functionality, such as acetophenone or benzaldehyde, formed $(M + 15)^+$ ions. The DME reactions were also selective for disubstituted aromatic compounds. Generally, meta and para disubstituted aromatic substrates containing at least one carbonyl functional group formed $(M + 15)^+$ adducts, whereas those compounds not containing a carbonyl group or having substituents located in ortho positions formed $(M + 13)^+$ ions. The $CH_3\overset{+}{O}HCH_3$-reactive ions resulted in protonated aromatic ions in the quadrupole ion trap. In the conventional ion source, the DME reactions were less selective, and a mixture of $(M + H)^+$, $(M + 13)^+$, $(M + 15)^+$, $(M + 45)^+$, and $(M + 47)^+$ adducts were formed for each aromatic substrate.

To elucidate the basis for the functional group-selective methylene substitution reactions of DME observed in the quadrupole ion trap, an evaluation of the selective behavior of other methylene donating reactive species, including ions from ethylene (ET) and ETOX, was undertaken. CAD of the adduct ions provided insight into the mechanisms of formation of the methylene substitution ions. The ion chemistry of ETOX [20] and ET [21] has been studied previously, but the structural selectivity of adduct formation with substituted aromatic compounds has not been compared. In the current study, ion/molecule reactions between these three reagent gases and simple aromatics, including both monosubstituted and disubstituted oxyaromatics, have been investigated in detail to determine functional group selectivity. Additionally, the analytical utility of adduct formation is characterized by CAD experiments to determine the value of adducts as structurally diagnostic ions.

## Experimental

Ion/molecule reactions were examined by using a Finnigan-MAT (San Jose, CA) quadrupole ion trap mass spectrometer (ITMS) [22]. A typical ion/molecule reaction sequence was initiated with a short electron ionization pulse, after which a selected reagent ion was isolated by using the appropriate application of direct current (dc) and radiofrequency (rf) voltages. The dc voltages used to isolate an ion were typically $-40$ to $-100$ V, and the rf voltages were $\sim 100$ V at 1.1 MHz. The chosen reagent ion was then allowed to undergo ion/molecule reactions with the neutral analyte for a period of 10–1000 ms. The product ion spectrum was then recorded by using the mass-selective instability mode to eject ions from the trap onto an electron multiplier. Alternatively, reagent ions were allowed to react with neutral aromatics, and then a particular product ion was isolated prior to collisional activation. Collisional activation involved the application of an alternate current voltage of 0.1–1.0 V at the axial frequency of motion of the ion of interest (typically 500 kHz). Typical reagent gas pressures were nominally $1 \times 10^{-5}$ torr, and helium buffer gas pressure was 0.8 mtorr. Aromatic compounds were introduced via a leak valve to $8 \times 10^{-7}$ torr. Typical ion/molecule reaction times were 50 ms, activation times were 4 ms, and activation voltages were $\sim 0.5$ V. When using ET as the reactive gas, the intensities of the ET ions of $m/z$ 28 and $m/z$ 29 rapidly decay after 1 ms as the abundances of $m/z$ 41, 67, and 69 increase with time. The propenyl ion at $m/z$ 41 reacts to produce $C_5H_7^+$ ($m/z$ 67) and $C_5H_9^+$ ($m/z$ 69) [21] at longer times. For ETOX reactions, the reagent ion population is composed of a variety of ions including $m/z$ 15, 28, 29, 42, 43, and 44 at storage times $< 2$ ms. At longer times, protonated ETOX and $(ETOX + 13)^+$ dominate.

For the comparative study, a Finnigan-MAT TSQ-70 triple stage quadrupole mass spectrometer [23] equipped with a conventional CI source was utilized with reagent gas pressure set at nominally 1 torr. For CAD experiments, the collision energy was 20 V, and the collision gas (argon) pressure was 2 mtorr in the second quadrupole. Multiple collisions occur under these conditions. For ET ion/molecule reactions, a pressure of 1150 mtorr was used in the ion source. The major reactive ions formed include $m/z$ 27, 28, 29, 39, 41, 53, and 55, with $m/z$ 41 the most abundant ion. The reagent ion population is pressure dependent, and the pressure was set to optimize the formation of adduct ions. With ETOX as the reactive gas, the reagent ion population in a conventional ion source at 1200 mtorr pressure consists predominantly of $m/z$ 45.

## Results and Discussion

To compare the selectivity of ion/molecule reactions of ETOX, ET, and DME, a variety of monosubstituted and disubstituted aromatic compounds were used as substrates. First, the reaction chemistry of ET and ETOX is briefly described, then a survey of these ion/molecule reaction results is presented in the following sections to highlight the differences observed for the different reagents and substrates. CAD is then used to obtain a more detailed structural characterization of the adduct ions for four of the monosubstituted aromatic compounds (phenol, anisole, benzaldehyde, and acetophenone), and two disubstituted aromatic compounds (meta-anisaldehyde and para-hydroxyacetophenone). From these results, conclusions will be drawn about the selectivity of methylene substitution and the diagnostic value of related adducts.

### *Reactions with Ethylene and Ethylene Oxide Ions*

The reactive ion from ET is observed at $m/z$ 41, the allyl cation. The products of reactions of this species with selected aromatic molecules in the ITMS are shown in Table 1. The abundances of the various products are time dependent, and the most abundant ion is always $(M + H)^+$. Similar to the reactions of the DME reagent ions, protonation and formation of $(M + 13)^+$ are major reactions, although the propensity for methylene substitution does not follow the same selectivity trends as was observed for DME. Additionally, in some cases adducts are seen at $(M + 27)^+$ and $(M + 41)^+$. There is no obvious pattern based on substituent selectivity for the appearance of $(M + 13)^+$, $(M + 27)^+$, or $(M + 41)^+$.

In the conventional ion source, adduct ions from ion/molecule reactions with aromatic substrates and ET are observed at $(M + H)^+$, $(M + 13)^+$, $(M + 29)^+$, $(M + 41)^+$, and $(M + 55)^+$, and the abundances of these ions are also pressure dependent. For each aromatic substrate, typically the $(M + H)^+$ ion represents ~ 75–80% of the total ion current, the $(M + 13)^+$ contributes 3–5%, the $(M + 29)^+$ contributes 2–3%, the $(M + 41)^+$ ion represents 10–20%, and the $(M + 55)^+$ ion contributes < 5%. Reactions in the conventional ion source show no selectivity for functional groups of the aromatic substrates.

For ETOX, the dominant reactive species in the ITMS are at $m/z$ 45 $(ETOX + H)^+$, and $m/z$ 57 $(ETOX + 13)^+$. Isolation of $m/z$ 45 and subsequent reactions with the aromatics in the ITMS results in formation of $(M + H)^+$, $(M + 13)^+$, $(M + 27)^+$, and $(M + 29)^+$ (Table 2), whereas isolation and reaction of $m/z$ 57 results only in production of $(M + H)^+$ ions. The formation of the various adduct ions for the aromatic compounds do not follow an obvious pattern based on substituent selectivity, nor does the formation of $(M + 13)^+$ duplicate the selectivity trends observed for the formation of $(M + 13)^+$ using DME or ET.

Reactions with ETOX ions and the aromatic compounds in the conventional ion source yield abundant $(M + H)^+$ and $(M + 45)^+$ adducts with minor abundances of $(M + 13)^+$ and $(M + 27)^+$ adducts. Typically, the $(M + H)^+$ ion contributes 50% of the ion current, the $(M + 13)^+$ and $(M + 27)^+$ ions represent a total of 5–10%, and the remaining 40% of the ion current is due to $(M + 45)^+$. Reactions in the conventional ion source show no selectivity for functional groups of the aromatic substrates.

### *Characterization of Aromatic Adduct Ion Structures*

The structures of adduct ions of phenol, anisole, benzaldehyde, and acetophenone, all monosubstituted aromatic compounds, were characterized by using low energy CAD in a triple quadrupole mass spectrometer and a quadrupole ITMS. The spectra

**Table 1.** Adduct formation with ET ions in an ITMS

| Compound | $(M + 1)^+$ | $(M + 13)^+$ | $(M + 27)^+$ | $(M + 41)^+$ |
|---|---|---|---|---|
| Benzene | + | + | + | NO |
| Anisole | + | + | NO | + |
| Phenol | + | + | + | NO |
| Benzaldehyde | + | + | + | + |
| Acetophenone | + | + | NO | NO |
| Vanillin | + | + | NO | NO |
| 2-Anisaldehyde | + | + | NO | NO |
| 2-Hydroxyacetophenone | + | NO | NO | NO |
| 4-Hydroxyacetophenone | + | NO | NO | NO |
| 4-Methoxyacetophenone | + | NO | NO | NO |

**Table 2.** Adduct formation with ETOX ions in an ITMS

| Compound | $(M + 1)^+$ | $(M + 13)^+$ | $(M + 27)^+$ | $(M + 29)^+$ |
|---|---|---|---|---|
| Benzene | + | + | + | NO |
| Anisole | + | + | + | + |
| Phenol | + | + | NO | NO |
| Acetophenone | + | + | NO | + |
| 4-Methoxyacetophenone | + | + | NO | + |
| Vanillin | + | + | NO | NO |
| 2-Anisaldehyde | + | NO | NO | NO |
| Methyl benzyl ether | + | + | NO | + |
| 4-Hydroxyacetophenone | + | + | NO | + |
| 2-Hydroxyacetophenone | + | + | NO | NO |

obtained with each spectrometer are qualitatively similar. These particular aromatic compounds were selected because they contain functional groups that are common to the more complex aromatic systems. Described below are the CAD behaviors of the various product ions from ion/molecule reactions of the ET, ETOX, and DME ions with aromatic substrates. The $(M + H)^+$ and $(M + 13)^+$ ions are described first because all the reagent gases induced formation of these products. Then the structures of the adducts specific to each reagent gas are discussed in separate sections.

*$(M + H)^+$ and $(M + 13)^+$ adducts.* Each of the reagent gases induced formation of $(M + H)^+$ and $(M + 13)^+$ ions in the conventional ion source. Collisional activation of the protonated ions formed using each of the three different reactive gases indicates that the CAD mass spectra are identical, regardless of which reactive gas was used for ionization. The most predominant dissociation routes are listed in Table 3.

Likewise, the $(M + 13)^+$ ions that are formed for each aromatic substrate using each of the reagent gases are indistinguishable by CAD. This suggests that either the collisional activation process causes complete isomerization of different ion structures so that initial structural differences are eliminated, or the multiple collisions that occur in the ion source favor formation of the most thermodynamically favorable $(M + 13)^+$ products prior to collisional activation (and therefore all have the same initial structure). Deuterium labeling studies [19] have shown that the formation of the $(M + 13)^+$ ions for anisole and phenol does not involve substituent attachment but rather formation of an alkyl substituted aromatic structure (as shown in the mechanism discussed earlier). The CAD results are shown in Table 3. The $(M + 13)^+$ adducts do not necessarily dissociate via the same pathways that are observed for the $(M + H)^+$ ions. For example, protonated phenol dissociates predominantly via dehydration whereas the $(M + 13)^+$ ion dissociates via loss of CO and $CH_2O$. The CAD spectra for the other aromatic ions also exhibit significant distinctions.

*$(M + 45)^+$ and $(M + 47)^+$ adducts from DME.* The CAD results for the $(M + 45)^+$ and $(M + 47)^+$ ions formed via reactions of DME ions with phenol, anisole, benzaldehyde, and acetophenone are shown in Table 4. The $(M + 47)^+$ adducts dissociate only by elimination of neutral DME, resulting in formation of $(M + H)^+$. This suggests that the $(M + 47)^+$ adducts are loose proton-bound dimers of DME and the aromatic substrate. Cleavage at the proton bridge yields the thermochemically favored product ion. The species of higher proton affinity retains the proton, and the other species is expelled as a neutral. Because the proton affinity of DME is only 192.1 kcal/mol [24], whereas the proton affinities of the aromatic substrates are substantially higher (shown in Table 3), in each case the proton is retained by the aromatic portion, resulting in $(M + H)^+$.

The CAD results of the $(M + 45)^+$ adducts include a variety of fragments, indicating that these are not loosely bound dimer species (see Table 4). The dissociation routes that are typically observed include: (1) elimination of $CH_3OH$, resulting in the $(M + 13)^+$ ion (observed for phenol and anisole), (2) elimination of $CH_2O$, resulting in the $(M + 15)^+$ ion (observed for acetophenone), and (3) formation of $m/z$ 45, by simple cleavage of the DME ionic portion from the aromatic substrate (observed for all of the aromatic substrates). The first two processes imply that the $(M + 45)^+$ adducts are precursors to the methylene substitution products at $(M + 13)^+$ and the methyl addition products at $(M + 15)^+$.

*$(M + 41)^+$ adducts from ET.* Reactions of ET ions with the four aromatic compounds result in $(M + 41)^+$

**Table 3.** CAD spectra of $(M + H)^+$ and $(M + 13)^+$ of monosubstituted aromatic ions

| Compound (PA)[a] Adduct, $m/z$ | Daughter ions (neutral loss) | | | |
|---|---|---|---|---|
| Phenol (196.3) | | | | |
| $(M + H)^+$, 95 $^+$ | 77 $^+$(-$H_2O$) | | | |
| $(M + 13)^+$, 107 $^+$ | 77 $^+$(-$CH_2O$) | 79 $^+$(-CO) | | |
| Anisole (200.3) | | | | |
| $(M + H)^+$, 109 $^+$ | 94 $^+$(-$CH_3$) | 79 $^+$(-$CH_2O$) | 77 $^+$(-$CH_3OH$) | |
| $(M + 13)^+$, 121 $^+$ | 106 $^+$(-$CH_3$) | 91 $^+$(-$CH_2O$) | 77 $^+$(-$C_2H_4O$) | |
| Benzaldehyde (200.2) | | | | |
| $(M + H)^+$, 107 $^+$ | 79 $^+$(-CO) | 77 $^+$(-$CH_2O$) | | |
| $(M + 13)^+$, 119 $^+$ | 91 $^+$(-CO) | | | |
| Acetophenone (205.4) | | | | |
| $(M + H)^+$, 121 $^+$ | 106 $^+$(-$CH_3$) | 43 $^+$(-$C_6H_6$) | | |
| $(M + 13)^+$, 133 $^+$ | 115 $^+$(-$H_2O$) | 105 $^+$(-CO) | 103 $^+$(-$CH_2O$) | 77 $^+$(-$C_3H_4O$) |

[a] Proton affinity in kcal/mol [24].

**Table 4.** CAD spectra of $(M + 45)^+$ and $(M + 47)^+$ adducts of DME

| Compound (f. wt.) Adduct, $m/z$ | Daughter ions (neutral loss) | | |
|---|---|---|---|
| Phenol (94) | | | |
| $(M + 45)^+$, $139^+$ | $45^+(-C_6H_5OH)$ | $107^+(-CH_3OH)$ | |
| $(M + 47)^+$, $141^+$ | $95^+(-CH_3OCH_3)$ | | |
| Anisole (108) | | | |
| $(M + 45)^+$, $153^+$ | $45^+(-C_6H_5OCH_3)$ | $107^+(-CH_3OCH_3)$ | $121^+(-CH_3OH)$ |
| $(M + 47)^+$, $155^+$ | $109^+(-CH_3OCH_3)$ | | |
| Benzaldehyde (106) | | | |
| $(M + 45)^+$, $151^+$ | $45^+(-C_6H_5COH)$ | $105^+(-CH_3OCH_3)$ | |
| $(M + 47)^+$, $153^+$ | $107^+(-CH_3OCH_3)$ | | |
| Acetophenone (120) | | | |
| $(M + 45)^+$, $165^+$ | $45^+(-C_6H_5COCH_3)$ | $119^+(-CH_3OCH_3)$ | $135^+(-CH_2O)$ |
| $(M + 47)^+$, $167^+$ | $121^+(-CH_3OCH_3)$ | | |

ions in addition to the $(M + H)^+$ and $(M + 13)^+$ adducts already discussed. The CAD mass spectra of these adducts are listed in Table 5. Based on reagent ion isolation and CAD experiments, the $(M + 41)^+$ adduct is a precursor to the $(M + 13)^+$ adduct. The reactive ion of $m/z$ 41 was isolated and allowed to react with a chosen aromatic compound. The adduct ion, $(M + 41)^+$, was then isolated and collisionally activated. The predominant dissociation pathway is via loss of 28 u, ET elimination, and results in formation of $(M + 13)^+$. A mechanism is proposed:

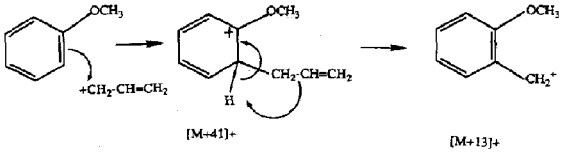


It has not been determined if the methylene addition occurs at the ortho, meta, or para positions, or if the substitution involves ring expansion.

In addition to formation of $(M + 13)^+$, the $(M + 41)^+$ ions dissociate via pathways that suggest that they are a mixture of covalently bound addition products and loosely bound complexes. For example, as shown in Table 5, the $(M + 41)^+$ ions for phenol and anisole dissociate after collisional activation to form $(M + H)^+$ ions via net loss of allene ($C_3H_4$) and to form $(M + 13)^+$ via loss of ET ($C_2H_4$). This is consistent with the proposal that in the ion source the $(M + 41)^+$ complex is a direct precursor to both $(M + H)^+$ and $(M + 13)^+$ ions. To highlight the similarities and differences in the CAD spectra for the various adducts generated via reactions with ET ions, an example of the CAD mass spectra of $(M + 41)^+$, $(M + 13)^+$, and $(M + H)^+$ is shown for anisole in Figure 1.

*$(M + 45)^+$ adducts of ETOX.* Reactions of ETOX ions with the four aromatic compounds result in $(M + 45)^+$ adducts in addition to the $(M + H)^+$ and $(M + 13)^+$ ions already discussed. These $(M + 45)^+$ adducts are evidently loosely bound complexes because the CAD mass spectra reveal that the only operative dissociation route is by loss of $C_2H_4O$, resulting in $(M + H)^+$ ions via cleavage of the proton bridge. ETOX has a proton affinity of only 187.9 kcal/mol [24], well below that of the aromatic compounds, so formation of $(M + H)^+$ is thermochemically favored over the formation of $(ETOX + H)^+$. The absence of alternative dissociation routes of the $(M + 45)^+$ adducts suggests that the $(M + 13)^+$ ions are formed from a facile cleavage of a transient $(M + 45)^+$ complex that is not stabilized enough to survive in the ion source, and thus cannot be identified as a direct precursor to the $(M + 13)^+$ adducts.

In summary, it is apparent that the $(M + 45)^+$ adducts from DME are covalently bound precursors to $(M + 13)^+$ or $(M + 15)^+$ ions, whereas the $(M + 47)^+$ adducts are loosely bound complexes. The $(M + 41)^+$ adducts of ET appear to be precursors to $(M + 13)^+$ and $(M + H)^+$ ions. Finally, the $(M + 45)^+$ adducts of ETOX are loosely bound complexes. No stable precursors to the $(M + 13)^+$ are observed. Evaluation of the CAD spectra for each type of adduct indicates that the loosely bound complexes give little information about the nature of the aromatic substrate, but the CAD spectra for both the $(M + H)^+$ and $(M + 13)^+$ ions provide relevant structurally diagnostic features.

**Table 5.** CAD spectra of $(M + 41)^+$ ions of ET

| Compound (f. wt.) Adduct, $m/z$ | Daughter ions (neutral loss) | |
|---|---|---|
| Phenol (94) | | |
| $135^+$ | $107^+(-C_2H_4)$ | $95^+(-C_3H_4)$ |
| Anisole (108) | | |
| $149^+$ | $121^+(-C_2H_4)$ | $109^+(-C_3H_4)$ |
| Benzaldehyde (106) | | |
| $147^+$ | $105^+(-C_3H_6)$ | $91^+(-C_2H_4 + CO)$ |
| Acetophenone (120) | | |
| $161^+$ | $133^+(-C_2H_4)$ | $43^+(-C_6H_6 + C_3H_4)$ |

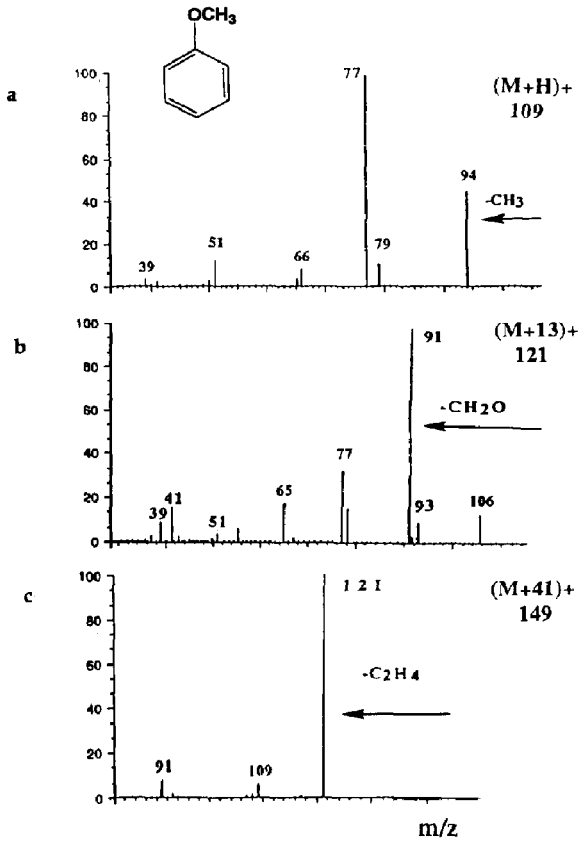


**Figure 1.** CAD spectra of (a) $(M + 1)^+$, (b) $(M + 13)^+$, and (c) $(M + 41)^+$ from reactions of ET and anisole in the TQMS.

*Disubstituted aromatic compounds.* The adduct ions of two disubstituted aromatic compounds were characterized via CAD to correlate the importance of each substituent on the resulting reaction and dissociation behavior. Para-hydroxyacetophenone and meta-anisaldehyde were chosen as the models because they incorporate the functional groups of the simple mono-substituted aromatic compounds discussed above.

Ion/molecule reactions of dimethyl ether ions with para-hydroxyacetophenone result in four ion/molecule reaction products: $(M + H)^+$, $(M + 15)^+$, $(M + 45)^+$, and $(M + 47)^+$. The ions in the CAD mass spectra are listed in Table 6. The protonated ion dissociates only via formation of acetyl ion, $m/z$ 43, the same significant fragment ion observed for protonated acetophenone. The methylated ions dissociate via two predominant pathways: elimination of $CH_2O$ and formation of acetyl ion. Both routes were observed for the $(M + 15)^+$ adduct of acetophenone [19]. To a lesser extent, the $(M + 15)^+$ adduct also dissociates via elimination of $CH_3$., a pathway that was noted for dissociation of $(M + 15)^+$ of phenol. Thus, it appears that either substituent may mediate the dissociation behavior of the $(M + 15)^+$ adduct.

With ET as the reactive CI gas, para-hydroxyacetophenone forms $(M + H)^+$ and $(M + 41)^+$ ions. The types of fragment ions observed in the CAD spectrum of the $(M + 41)^+$ adducts suggest that the acetyl substituent mediates the favorable dissociation routes.

For meta-anisaldehyde, $(M + H)^+$, $(M + 13)^+$, $(M + 45)^+$, and $(M + 47)^+$ ions are formed with DME as the reactive gas; $(M + H)^+$, $(M + 13)^+$, and $(M + 41)^+$ adducts are formed with ET; and $(M + H)^+$, $(M + 13)^+$, and $(M + 45)^+$ are produced with ETOX as the reactive gas. The ions in the CAD spectra of these adducts are listed in Table 7. For the $(M + H)^+$ and $(M + 13)^+$ ions (from any reactive gas), and the $(M + 41)^+$ ion from ET, the fragment ions observed in the CAD spectra of these adducts indicate that both substituents mediate the dissociation routes. However, the CAD spectrum for the $(M + 45)^+$ adduct from DME indicates that the carbonyl substituent has the more significant influence on the dissociation behavior. The $(M + 47)^+$ ions (from DME) and the $(M + 45)^+$ (from ETOX) are loose complexes that dissociate to $(M + H)^+$ upon cleavage of the weak proton bridge. To assist in visualization of the similarities and differences observed in the CAD spectra of the various adducts, a series of CAD mass spectra for the successive dissociation of $(M + 41)^+$, $(M + 13)^+$, and $(M + H)^+$ adducts from reactions of ET ions with meta-anisaldehyde is shown in Figure 2.

In general, the formation and dissociation of adducts of the disubstituted aromatic compounds with DME, ETOX, and ET can be rationalized based on comparisons to the CAD mass spectra recorded for the adduct ions of the monosubstituted aromatic substrates. Most of the dissociation pathways observed

**Table 6.** CAD spectra of adducts of para-hydroxyacetophenone

| Adduct | Parent, $m/z$ | Daughter ions (neutral loss) | | |
|---|---|---|---|---|
| $(M + H)^+$ | $137^+$ | $43^+$ | | |
| $(M + 15)^+$ | $151^+$ | $136^+(-CH_3\cdot)$ | $121^+(-CH_2O)$ | $43^+$ |
| $(M + 45)^+$/DME | $181^+$ | $151^+(-CH_2O)$ | $149^+(-CH_3OH)$ | $45^+$ |
| $(M + 47)^+$/DME | $183^+$ | $137^+(-CH_3OCH_3)$ | $43^+$ | |
| $(M + 41)^+$/ET | $177^+$ | $159^+(-H_2O)$ | $43^+$ | |
| $(M + 45)^+$/ETOX | $181^+$ | $137^+(-C_2H_4O)$ | $43^+$ | |

**Table 7.** CAD spectra of adducts of meta-anisaldehyde

| Adduct | Parent, *m/z* | Daughter ions (neutral loss) | | |
|---|---|---|---|---|
| $(M + H)^+$ | $137^+$ | $109^+$(-CO) | $94^+$(-CO + $CH_3$) | $77^+$ |
| $(M + 13)^+$ | $149^+$ | $134^+$(-$CH_3$·) | $121^+$(-CO) | $91^+$(-CO + $CH_2O$) |
| $(M + 15)^+$ | $151^+$ | $136^+$(-$CH_3$·) | $123^+$(-CO) | $121^+$(-$CH_2O$) |
| | | $108^+$(-CO + $CH_3$) | $91^+$ | |
| $(M + 45)^+$/DME | $181^+$ | $151^+$(-$CH_2O$) | $135^+$(-$CH_3OCH_3$) | $45^+$ |
| $(M + 47)^+$/DME | $183^+$ | $137^+$(-$CH_3OCH_3$) | $109^+$(-$CH_3OCH_3$ + CO) | |
| | | $47^+$ | | |
| $(M + 41)^+$/ET | $177^+$ | $149^+$(-$C_2H_4$) | $135^+$(-$C_3H_6$) | |
| | | $121^+$(-$C_2H_4$ + CO) | | |
| $(M + 45)^+$/ETOX | $181^+$ | $137^+$(-$C_2H_4O$) | $109^+$(-$C_2H_4O$ + CO) | |
| | | $94^+$ | $77^+$ | |

for the adducts are analogous to those observed for the monosubstituted aromatic adducts. It appears, however, that for the $(M + 45)^+$ adducts formed with DME and the $(M + 41)^+$ adduct formed with ET, the presence of a carbonyl functional group has the more significant influence on the resulting dissociation behavior than the presence of a hydroxy or methoxy group.

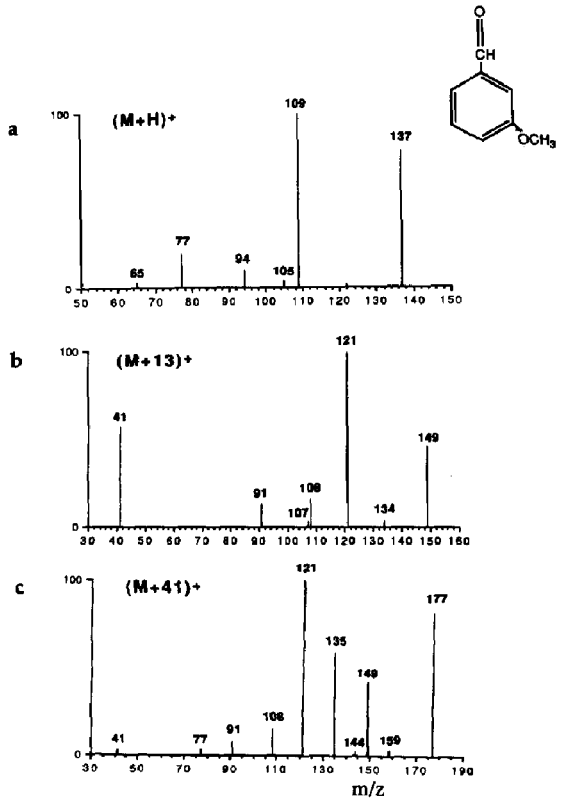


**Figure 2.** CAD spectra of (A) $(M + H)^+$, (B) $(M + 13)^+$, and (C) $(M + 41)^+$ from reactions of ET and meta-anisaldehyde in the TQMS.

## *Selectivity of Methylene Substitution*

Two points about the methylene substitution selectivity need to be addressed. First, the methylene substitution selectivity is only observed using DME ions, and not with ETOX or ET ions. Second, the methylene substitution selectivity is only observed in the quadrupole ion trap environment, but not in the higher pressure conventional ion source. When using $CH_3OCH_2^+$ from DME to promote the methylene substitution reactions in the quadrupole ion trap, only phenol and anisole form $(M + 13)^+$, not acetophenone or benzaldehyde. For acetophenone and benzaldehyde, $(M + 15)^+$ ions are observed instead. When using $CH_2 = CHCH_2^+$ from ET or $(ETOX + H)^+$ from ETOX to promote methylene substitution reactions in the quadrupole ion trap, all of the monosubstituted aromatic compounds produce $(M + 13)^+$ ions.

The exothermicities of the different methylene substitution reactions were calculated from estimated heats of formation of the reactants and heats of formation of the products [24]. In general, the overall exothermicities for the methylene substitution reactions involving the $CH_2 = CHCH_2^+$ and $(ETOX + H)^+$ ions are about 8–10 kcal/mol more exothermic than the corresponding reactions involving $CH_3OCH_2^+$. Additionally, methyl addition is a competitive exothermic process accessible to the $CH_3OCH_2^+$ ions, which is not an available reaction channel for the reactive $CH_2 = CHCH_2^+$ and $(ETOX + H)^+$ ions. The methoxy and hydroxy substituents are electron-donating groups and enhance the electrophilic substitution of the aromatic ring. However, the aromatic compounds with electron withdrawing substituents, i.e., the carbonyl-containing ones, deactivate the electrophilic addition process. This latter effect makes the methylene substitution reaction less exothermic than

the methyl addition reaction for acetophenone and benzaldehyde.

Thus, based on the overall substituent-directed favorabilities of the electrophilic aromatic additions coupled with the exothermicities of the reactions, it is possible to categorize the selectivity of methylene substitution of the three reactive species, $CH_3OCH_2^+$, $CH_2 = CHCH_2^+$, $(ETOX + H)^+$. The methylene-donating ions generated from ET or ETOX undergo reactions with the aromatic substrates that are more exothermic, and thus are better able to drive the methylene substitution process for all the aromatic compounds, regardless of the electron-donating or releasing capabilities of the substituents. For the reactive ions from DME, the methylene substitution reactions are less exothermic, and simple methyl transfer is a competing process. The differences in selectivity noted between the low pressure quadrupole ion trap environment and the higher pressure conventional ion source are attributed to the reduced collision frequency in the ion trap which reduces the extent of collisional stabilization of adduct ions.

## Conclusions

Of the reactive gases examined, dimethyl ether demonstrates the greatest functional group and positional selectivity for ion/molecule reactions with oxyaromatic compounds. Overall, both ET and ETOX produce a variety of adduct ions, but the methylene substitution reactions with these reactive species are not selective as they are with DME. Differences in reaction exothermicities and competitive reactions account for the differences observed in selectivity of the methylene substitution reagents in the quadrupole ion trap. Dimethyl ether ions follow two competitive exothermic reaction routes with the aromatic substrates, methyl addition and methylene substitution, so the observed product ions reflect the substituent properties of the aromatic substrates. Those substrates with electron-releasing substituents favor the methylene substitution pathway, whereas the substrates with electron-withdrawing substituents favor the methyl addition pathway.

ET-reactive ions induce predominantly proton transfer reactions, and only relatively minor (total of 10–20%) amounts of adduct ions $(M + 13)^+$ and $(M + 41)^+$ are formed. Ethylene oxide-reactive ions produce abundant $(M + 45)^+$ adduct ions in addition to the $(M + 13)^+$ ions, but the $(M + 45)^+$ adduct ions provide little structural insight into the nature of the aromatic substrate. The structures of the adducts mentioned above, $(M + 45)^+$, $(M + 41)^+$, were characterized by using low energy CAD, and the adducts proved to be either simple proton-bound dimers or covalently bound adducts that were precursors to other adducts.

The results of this study suggest several more general conclusions about developing a rational approach to finding alternative CI agents. First, the low pressure environment of the quadrupole ion trap offers more flexibility for developing selective ion/molecule reaction strategies than the higher pressure environment of a conventional ion source. Second, reactive ions that have competitive ion/molecule reaction routes are more likely to induce selective behavior than those reactive species that follow only one dominant reaction pathway.

## Acknowledgments

This work was supported by the Welch Foundation (F-1155), the National Science Foundation (Postdoctoral Starter Grant), the Society of Analytical Chemists of Pittsburgh, and an ASMS Young Investigator Award.

## References

1. Munson, B.; Field, F. *J. Am. Chem. Soc.* **1966**, 2621.
2. Harrison, A. *Chemical Ionization Mass Spectrometry*, CRC Press: Boca Raton, FL. 1983.
3. Vairamani, M.; AliMirza, A.; Sriniva, R. *Mass Spectrom. Rev.* **1990**, *9*, 235.
4. Richter, W. J.; Schwarz, H. *Angew. Chem. Int. Ed. Engl.* **1978**, *17*, 424.
5. Bartmess, J. E. *Mass Spectrom. Rev.* **1989**, *8*, 297.
6. Budzikiewicz, H.; Laufenberg, G.; Brauner, A. *Org. Mass Spec.* **1985**, *20*, 65.
7. Hunt, D.; Harvey, T. *Anal. Chem.* **1975**, *47*, 2136.
8. Ferrer-Correia, A.; Jennings, K.; Sharma, D. *Org. Mass Spectrom.* **1976**, *11*, 867.
9. Orlando, R.; Strobel, F.; Ridge, D.; Munson, B. *Org. Mass Spectrom.* **1987**, *22*, 597.
10. Lange, C. *Org. Mass Spectrom.* **1986**, *21*, 524.
11. Wang, S.; Sah, Y.; Xu, S.; Pan, J. *Anal. Chem.* **1985**, *57*, 2283.
12. Dzidic, I. *J. Am. Chem. Soc.* **1972**, 8333.
13. Keough, T. *Anal. Chem.* **1982**, *154*, 2540.
14. Lane, D.; McGuire, M. *Org. Mass Spectrom.* **1983**, *18*, 494.
15. Freiser, B. *Talanta* **1985**, *32*, 697.
16. Burnier, R.; Byrd, G.; Freiser, B. *Anal. Chem.* **1980**, *52*, 1641.
17. Peake, D.; Gross, M. *Anal. Chem.* **1985**, *57*, 115.
18. Bjarnason, A.; Taylor, J.; Kinsinger, J.; Cody, R.; Weil, D. *Anal. Chem.* **1989**, *61*, 1889.
19. Brodbelt, J.; Liou, J.; Donovan, T. *Anal. Chem.* **1991**, *63*, 1205.
20. Coderman, R. R.; LeBreton, R. R.; Butrill, S. E.; Williamson, A. D.; Beauchamp, J. L. *J. Chem. Phys.* **1976**, *65*, 4929.
21. Herod, A. A.; Harrison, A. G. *Int. J. Mass Spectrom. Ion Phys.* **1970**, *415*, 431.
22. Louris, J. L.; Cooks, R. G.; Syka, J. E. P.; Kelley, P. E.; Stafford, G. C.; Todd, J. F. *Anal. Chem.* **1987**, *59*, 1677.
23. Slayback, J.; Story, M. *Ind. Res. Dev.* Feb. **1981**, 129.
24. Lias, S. G.; Liebman, J. F.; Levin, R. D. *J. Phys. Chem. Ref. Data* **1984**, *13*.